THE JOURNAL OF BIOLOGICAL CHEMISTRY VOL. 290, NO. 17, pp. 10703–10716, April 24, 2015
Published in the U.S.A.

Constitutive Phosphorylation of Cardiac Myosin Regulatory Light Chain *in Vivo*[*]

Received for publication, January 29, 2015, and in revised form, February 25, 2015 Published, JBC Papers in Press, March 2, 2015, DOI 10.1074/jbc.M115.642165

Audrey N. Chang[‡], Pavan K. Battiprolu[§], Patrick M. Cowley[¶‖], Guohua Chen[‡], Robert D. Gerard[**], Jose R. Pinto[‡‡], Joseph A. Hill[§], Anthony J. Baker[¶‖], Kristine E. Kamm[‡], and James T. Stull[‡1]**

From the Departments of [‡]Physiology, [§]Internal Medicine (Cardiology), and [**]Molecular Biology, University of Texas Southwestern Medical Center, Dallas, Texas 75390, the [¶]Veterans Affairs Medical Center, San Francisco, California 94143, the [‖]University of California, San Francisco, California 94143, and the [‡‡]Department of Biomedical Sciences, Florida State University College of Medicine, Tallahassee, Florida 32306

Background: Myosin regulatory light chain phosphorylation is necessary for normal cardiac performance.
Results: Regulatory light chain phosphorylation is not affected by conditions affecting phosphorylation of other sarcomeric proteins, including β-adrenergic tone.
Conclusion: Significant regulatory light chain phosphorylation in beating hearts is sustained physiologically by low cMLCK and MLCP activities.
Significance: Constitutive regulatory light chain phosphorylation stabilizes cardiac performance.

In beating hearts, phosphorylation of myosin regulatory light chain (RLC) at a single site to 0.45 mol of phosphate/mol by cardiac myosin light chain kinase (cMLCK) increases Ca^{2+} sensitivity of myofilament contraction necessary for normal cardiac performance. Reduction of RLC phosphorylation in conditional cMLCK knock-out mice caused cardiac dilation and loss of cardiac performance by 1 week, as shown by increased left ventricular internal diameter at end-diastole and decreased fractional shortening. Decreased RLC phosphorylation by conventional or conditional cMLCK gene ablation did not affect troponin-I or myosin-binding protein-C phosphorylation *in vivo*. The extent of RLC phosphorylation was not changed by prolonged infusion of dobutamine or treatment with a β-adrenergic antagonist, suggesting that RLC is constitutively phosphorylated to maintain cardiac performance. Biochemical studies with myofilaments showed that RLC phosphorylation up to 90% was a random process. RLC is slowly dephosphorylated in both noncontracting hearts and isolated cardiac myocytes from adult mice. Electrically paced ventricular trabeculae restored RLC phosphorylation, which was increased to 0.91 mol of phosphate/mol of RLC with inhibition of myosin light chain phosphatase (MLCP). The two RLCs in each myosin appear to be readily available for phosphorylation by a soluble cMLCK, but MLCP activity limits the amount of constitutive RLC phosphorylation. MLCP with its regulatory subunit MYPT2 bound tightly to myofilaments was constitutively phosphorylated in beating hearts at a site that inhibits MLCP activity. Thus, the constitutive RLC phosphorylation is limited physiologically by low cMLCK activity in balance with low MLCP activity.

Contractile proteins of the heart are highly organized in myofibrils containing sarcomeres. Contraction of the cardiac sarcomere initiated by Ca^{2+} is dependent on the hydrolysis of ATP by cardiac myosin (1). Ca^{2+} dependence of myosin ATPase activity is conferred by the troponin complex, which regulates the availability of myosin binding sites on actin filaments (2). Contractile performance dependent on the actin-myosin system is modulated by phosphorylation of sarcomeric proteins, such as the troponin subunit troponin I (TnI)[2] in the actin thin filament as well as the myosin regulatory light chain (RLC) and myosin binding protein-C (MyBP-C), which are thought to control the position of myosin heads in the thick filament (3–5). Mutations in RLC, TnI, and MyBP-C are associated with cardiac myopathies, and changes in their phosphorylation are reported in human heart diseases, underscoring the importance of their modulatory roles (6, 7).

Animal models that express a non-phosphorylatable cardiac RLC have solidified the requirement of RLC phosphorylation for optimal cardiac performance (8, 9). RLCs are phosphorylated by distinct and dedicated MLCKs in each muscle type, including cardiac, skeletal, and smooth muscles (3). Biochemically, cardiac RLC is phosphorylated by all three MLCKs and also zipper-interacting kinase (3, 10). Selective ablation of the cardiac MLCK (cMLCK) gene, but not of the skeletal MLCK gene, decreases cardiac RLC phosphorylation from 0.45 to 0.10 mol of phosphate/mol of RLC, showing kinase-specific effects in the heart (3, 5, 9, 11–14). This attenuation results in decreased cardiac performance and dilation of the adult mouse heart, not unlike the results obtained with knock-in mutant mice containing a nonphosphorylatable cardiac RLC. Overex-

[*] This work was supported, in whole or in part, by National Institutes of Health Grants HL080536 (to J. T. S.), HL06296 (to R. D. G.), and HL103840 (to J. R. P.). This work was also supported by Department of Veterans Affairs Merit Review Award I01BX000740 (to A. J. B.), the Moss Heart Fund (to J. T. S.), and the Fouad A. and Val Imm Bashour Distinguished Chair in Physiology (to J. T. S.).

[1] To whom correspondence should be addressed. Tel.: 214-645-6058; Fax: 214-645-6049; E-mail: james.stull@utsouthwestern.edu.

[2] The abbreviations used are: TnI, troponin I; MLCK, myosin light chain kinase; cMLCK, cardiac MLCK; RLC, myosin regulatory light chain; MyBP-C, myosin binding protein-C; MLCP, myosin light chain phosphatase; MYPT1, myosin phosphatase targeting subunit-1; MYPT2, myosin phosphatase targeting subunit-2; ROCK1, RhoA-associated kinase-1; CKO, conventional cMLCK knock-out; CFM, conditional cMLCK knock-out; ANOVA, analysis of variance.

pression of MLCK in the heart increases the extent of RLC phosphorylation, which is associated with improvement of cardiac performance and attenuation of hypertrophic responses to stress (15, 16).

The MLCKs in smooth and skeletal muscles are Ca^{2+}/calmodulin-dependent. In the absence of Ca^{2+}, the kinases are inhibited by a regulatory segment C-terminal of the catalytic core containing distinct autoinhibitory and calmodulin binding sequences (3). The primary structure of cMLCK has greater than 90% sequence similarity with smooth and skeletal muscle MLCKs in its catalytic core and regulatory segment. Whether the activity of cMLCK is Ca^{2+}/calmodulin-dependent is unclear, given conflicting reports; however, there is agreement that its catalytic activity is low (17, 18). Although animal studies involving gene ablation have confirmed that cMLCK is the primary kinase responsible for phosphorylation of RLC in ventricular muscle (12), signaling mechanisms that regulate the kinase or MLCP affecting RLC phosphorylation have not been elucidated.

Physiologically, values of RLC phosphorylation result from the relative activities of MLCK and MLCP. MLCP is composed of a regulatory targeting subunit, a catalytic subunit, and a small subunit of unknown function (3). The myosin-targeting regulatory subunit for MLCP in striated muscles is MYPT2, which targets the catalytic subunit PP1cδ to myosin filaments (19). Similar to the MYPT1 in smooth muscles, phosphorylation of MYPT2 reduces MLCP activity toward RLC (20). Overexpression of MYPT2 in the heart causes a decrease in RLC phosphorylation due to accumulation of the catalytic subunit PP1cδ (21).

RLC phosphorylation is consistently reported as 0.40–0.50 mol of phosphate/mol of RLC in beating hearts from various mammals (22–24). Additionally, the maximal extent of RLC phosphorylation appears to be limited to 0.5 mol/mol, because it was not increased in hearts after β-adrenergic stimulation that increases $[Ca^{2+}]_i$ and myocardial contractility (25–27). We asked whether the extent of RLC phosphorylation is limited by negative cooperativity or steric constraints in myofibrils, resulting in a fast phosphorylation rate for 50% of RLC with a slower phosphorylation rate in the remaining 50% of RLC. These considerations are related to cardiac myosin being a dimer of two heavy chains, each containing an RLC as well as the complex structure of the sarcomere involving myosin heavy chains interacting with other sarcomeric proteins.

Hearts from conventional cMLCK knock-out mice have 0.10 mol of phosphate/mol of RLC (11, 12). To determine whether the dilated phenotype caused by cMLCK knockout is preceded by a loss of cardiac performance associated with decreased RLC phosphorylation and phosphorylation of other sarcomeric proteins, we developed a conditional gene ablation mouse model for an acute cMLCK knockout.

EXPERIMENTAL PROCEDURES

Animals—All procedures were performed in accordance with the Institutional Animal Care and Use Guidelines at University of Texas Southwestern Medical Center with all animal experimental procedures reviewed and approved by the Institutional Animal Care and Use Committee. Animals were housed under standard conditions in the rodent facility.

A conventional knock-out of cMLCK (CKO) was generated from the floxed mice described previously (12). Mice with floxed alleles were bred with the CAG-Cre transgenic line, which allowed for excision of the floxed allele irrespective of transmission of the CAG-Cre gene (28). Heterozygous animals that had the knock-out allele but not the CAG-Cre gene, *Mylk3*$^{+/-}$, were selected for subsequent breeding. A conditional knock-out model (CFM) was generated by crossing mice with the floxed allele with the tamoxifen-inducible MerCreMer transgenic line. Cre-positive WT littermates were used as controls. Mice were injected with 0.5 mg tamoxifen (intraperitoneally) for 5 consecutive days. All lines were back-crossed into the C57BL6 inbred WT line (Jackson Laboratory) for at least 5 generations. For all studies, 12–15-week-old male mice were used.

A conventional knockin of the R21C mutation in cardiac TnI was described previously (29). All protocols and experimental procedures were approved by the Institutional Animal Care and Use Committee of the University of Miami and the Florida State University following the National Institutes of Health Guide for the Care and Use of Laboratory Animals. R21C mice have a homozygous knock-in mutation in the *TNNI3* gene (encoding cardiac troponin I), which substitutes an arginine at residue 21 with cysteine (R21C) and completely prevents PKA-mediated phosphorylation of Ser-23/24 of cTnI (30). Hearts of knock-in mice and age-matched littermates were collected from anesthetized mice and snap-frozen in liquid nitrogen.

Force measurements with mouse cardiac trabeculae were performed with wild type mice (C57BL/6J; Jackson Laboratory) in the laboratory of Dr. Anthony J. Baker at the University of California, San Francisco. This institution is accredited by the American Association for the Accreditation of Laboratory Animal Care (Institutional PHS Assurance Number A3476-01). The study was approved by the Animal Care and Use Subcommittee of the San Francisco Veterans Affairs Medical Center (Protocol 13-013) and conformed to the National Institutes of Health Guide for the Care and Use of Laboratory Animals (revised 2011).

Echocardiography—Echocardiograms were performed on conscious, gently restrained mice using a Vevo 2100 system with a MS400C scan head. Left ventricular internal diameter at end-diastole (LVEDD) and end-systole (LVESD) were measured from M-mode recordings. The percentage of fractional shortening was calculated as ((LVEDD − LVESD)/LVEDD) × 100. Measurements of interventricular septum thickness, left ventricular internal diameter, and left ventricular posterior wall thickness were made from two-dimensional parasternal short axis views in diastole (31). All measurements were made at the level of papillary muscles.

Animal Protocols—Dobutamine (5 ng/g/min) was infused though the jugular vein of mice anesthetized with isoflurane. At the end of the treatment, whole hearts were immediately excised, and ventricles were snap-frozen with clamps prechilled in liquid nitrogen. All tissue collections were performed in the afternoon between 3:00 and 5:00 p.m. For propranolol-treated samples, mice were injected with 1 mg/kg propranolol (intraperitoneally) 20 min prior to heart excision.

Statistical Analyses—Data are expressed as mean ± S.E. Statistical evaluation was carried out in GraphPad Prism using an

unpaired Student's *t* test for two comparisons or paired *t* test for comparison of the same sample before and after treatment. Analysis of variance and Newman-Keuls post-test were used for multiple comparisons. Significance was accepted at a value of $p < 0.05$.

Immunoblots and Antibodies—Frozen ventricles were ground in liquid nitrogen, and an aliquot was thawed in 10% trichloroacetic acid containing 10 mM dithiothreitol. Precipitated protein was washed free of acid with three 5-min washes in ethyl ether and resuspended by vigorous agitation in urea sample buffer (8 M urea, 20 mM Tris base, 23 mM glycine, 0.2 mM EDTA, 10 mM dithiothreitol, pH 8.6) using an orbital shaker (IKA Vibrax VXR) set at 1400 rpm for 30 min at room temperature. Complete denaturation and solubilization was achieved by additional urea crystals and prolonged agitation until crystals did not dissolve. Protein samples were centrifuged at 10,000 × *g* for 2 min, and protein concentration in supernatant fractions was measured by a Bradford assay. Proteins (2–20 μg) were subjected to SDS-PAGE after boiling in Laemmli buffer and transferred to PVDF (Immobilon-P, Millipore) or nitrocellulose (Protran, Whatman) and blotted by standard procedures. The amount of protein loaded was optimized empirically for each antibody to ensure density measurements were proportional to the amount of protein.

Measurements of RLC phosphorylation in heart homogenates were performed by urea/glycerol-PAGE and immunoblotting, as described previously (32). The urea/glycerol-PAGE system separates phosphorylated RLC from non-phosphorylated RLC, allowing a direct quantitative measure of RLC phosphorylation in terms of the fraction of phosphorylated RLC to total RLC (nonphosphorylated plus phosphorylated). Because the separation results from a single phosphate, data may also be calculated as mol of phosphate/mol of RLC. Although it was reported that a small amount of cardiac RLC may be diphosphorylated (33), we found that the amount relative to monophosphorylated RLC was too small to reliably measure by quantitative immunoblotting. Briefly, polyacrylamide gels containing 40% glycerol were pre-electrophoresed for 1 h at 400 V at room temperature in a minigel apparatus. Reservoir buffer contained 20 mM Tris base and 23 mM glycine, pH 8.6; thioglycolate and dithiothreitol (2.3 mM each) were included in the upper reservoir. Samples (2 μg of protein in urea sample buffer) were subjected to electrophoresis for 90 min at 400 V at room temperature and then transferred to a PVDF membrane for 1 h at 0.3 A at 4 °C. Post-transfer, proteins were fixed onto the PVDF membrane with 0.4% glutaraldehyde/PBS for 15 min at room temperature. The membrane was then rinsed three times in PBS and immunoblotted with antibody to cardiac RLC.

Antibodies to RLC, cMLCK, and skeletal MLCK were reported previously (12, 15). Polyclonal antibody raised against full-length cMLCK protein for cMLCK protein measurement studies was generated by the antibody production program at the Animal Resources Center at the University of Texas Southwestern Medical Center. Antibody to phosphorylated-phospholamban, pPLB_Thr17, were purchased from Badrilla Ltd.; antibody to cardiac pTnI_Ser23/24 (catalog no. 4004) was purchased from Cell Signaling Technology; and antibodies to total cardiac TnI (MAB1691), total PLB (05-205), and pPLB_Ser16 (07-052) were purchased from Millipore. Antibody to cardiac pMyBP-C_Ser282 (ALX 215-057) was purchased from Enzo Life. Antibody to total MYPT1 (residues 661–710) (LS-C117671) was purchased from LifeSpan BioSciences. Antibody to pMYPT1_Thr696 (ABS45) was purchased from Millipore. Polyclonal antibody for total MYPT2 was raised against mouse MYPT2 residues 673– 848 by Proteintech.

Cardiac Trabeculae—Male C57BL/6J mice (~13 weeks old) were anesthetized with sodium pentobarbital (100 mg/kg, intraperitoneally) and heparinized (100 units). Hearts were removed and immediately immersed in ice-cold arrest solution (120 mM NaCl, 30 mM KCl, 0.1 mM $CaCl_2$) and then perfused through the aorta with a modified Krebs-Henseleit solution (112 mM NaCl, 15 mM KCl, 1.2 mM $MgCl_2$, 10 mM glucose, 24 mM $NaHCO_3$, 1.2 mM Na_2SO_4, 2 mM $NaHPO_4$, 0.2 mM $CaCl_2$). The perfusate was oxygenated with 95% O_2, 5% CO_2 to give a pH of 7.4 at 22 °C. The free wall of right ventricle was removed from the heart, and a trabecula that was free running between the right ventricle wall and tricuspid valve was dissected. Trabeculae were ~1 mm long with an elliptical cross-section. The width, thickness, and cross-sectional area of trabeculae were 184.0 ± 18.6 μm, 136.5 ± 11.9 μm, and 0.022 ± 0.004 mm^2, respectively ($n = 19$). Trabeculae were placed in a muscle chamber (3 × 3 × 15 mm) and mounted on stainless steel pins with the valvular end attached to a micromanipulator and the ventricular end attached to a force transducer (AE-801, Kronex, Oakland, CA). Sarcomeres were observed using a ×40 objective, and sarcomere length was assessed using a video-based system (model 900B, Aurora Scientific, Inc., Ontario, Canada). Diastolic sarcomere length was set to 2.1 μm.

Trabeculae were equilibrated for 1 h in Krebs-Henseleit solution (5 ml/min) as described above, but with 5 mM KCl. The calcium level of the solution was increased to 2 mM in increments of 0.3 mM, and contractions were evoked by electrical field stimulation, using 4-ms square wave stimuli at supramaximal voltage. Trabeculae were subjected to one of the following conditions: 30 min of no electrical pacing, pacing at 0.5 Hz, or pacing at 1.5 Hz. The specimen was quickly removed from the apparatus and trimmed to remove the cube of ventricular wall and remnants of the valve. The sample was placed in 10% trichloroacetic acid and snap-frozen in liquid nitrogen. In some experiments, the phosphatase inhibitor, calyculin A (1 μM in DMSO; LC Laboratories, Woburn, MA), was added to the Krebs-Henseleit solution 30 min prior to pacing at 1.5 Hz. Precipitated trabeculae were then processed the same way as ground ventricles, described above.

Preparation of Cardiac Myofibrils and Myosin Filaments—Mouse cardiac myofibrils were prepared as reported previously (34). Native mouse cardiac myosin filaments were prepared from cardiac myofibrils as reported with minor modifications (35). Mouse ventricles were dissected, homogenized in 4 volumes of sucrose buffer relative to ventricular weight with a ground glass homogenizer, and collected by centrifugation (10,000 × *g*, 1 min) in a microcentrifuge tube. For all subsequent wash steps, the homogenate pellet was hand-homogenized with a plastic homogenizer directly in the microcentrifuge tube, and myofibrils were collected by low speed centrifugation (300 × *g*, 1 min). Myofibrils were washed two

times in wash buffer, two times in detergent buffer, and then four times in wash buffer. Washed myofibrils were resuspended in relaxing buffer (100 mM NaCl, 2 mM EGTA, 10 mM $MgCl_2$, 1 mM DTT, 10 mM imidazole, 5 mM Na_2ATP, pH 7.2) to the original 4 volumes for kinase assays. For native myosin filament preparation, washed myofibrils were directly resuspended in 48 μl of calpain-1 (Calbiochem) plus 1 μl of 0.1 M $CaCl_2$ and incubated at 30 °C for 30 min to cleave MyBP-C and dissociate thick and thin filaments. Calpain was inactivated with the addition of 100 μl of relaxing buffer plus 0.1 mM E64 protease inhibitor. Actin was depolymerized at room temperature for 30 min with 50 μl of unfractionated calcium-insensitive gelsolin fragments (1 mg/ml). Myosin filament volume was increased to 4 times ventricular weight with relaxing buffer and then used in phosphorylation studies. The intact nature of the myosin filaments and dissociation from thin filaments were confirmed by electron microscopy at the University of Texas Southwestern Electron Microscopy Facility.

Mass Spectrometry—Washed myofibrillar proteins from CKO mouse ventricles were separated by urea/glycerol-PAGE followed by E-Zinc reversible stain (Pierce). A band corresponding to phosphorylated RLC was excised from the gel and subjected to further separation by 15% SDS-PAGE, followed by staining with GelCode Blue Safe Protein Stain (Pierce). The RLC band was identified by size, excised from the gel and submitted to MS Bioworks, LLC (Ann Arbor, MI) for PTM profiling by nano-liquid chromatography (LC)/tandem MS (MS/MS) with a Waters NanoAcquity high pressure liquid chromatography system (Thermo Scientific, San Jose, CA). MS/MS-based peptide and protein identifications were accepted if they could be established at greater than 50% probability, and protein identifications were accepted if they could be established at greater than 90% and contained at least two identified peptides. Mascot was set up to search the Swissprot-mouse-reviewed. decoy database (33,292 entries), assuming the digestion enzyme trypsin. Mascot was searched with a fragment ion mass tolerance of 0.80 Da and a parent ion tolerance of 10.0 ppm. Carbamidomethyl of cysteine was specified in Mascot as a fixed modification. Deamination of asparagine and glutamine, oxidation of methionine, acetylation of the N terminus, and phosphorylation of serine, threonine, and tyrosine were specified in Mascot as variable modifications.

Phosphorylation of RLC in Cardiac Myofibrils and Native Myosin Filaments—For all kinase assays, RLC concentrations in myosin and myofibril preparations were calculated by mol of ^{32}P incorporated into samples maximally phosphorylated by skeletal muscle MLCK on the same day. Skeletal muscle MLCK was used because of its greater specific activity toward cardiac RLC relative to cMLCK. The optimal kinase concentration (80 nM for myofibrils, 10 nM for myosin filaments) used for temporal RLC phosphorylation studies was determined by titration with purified skeletal MLCK (0–150 nM). All reactions were performed at 25 °C in relaxing buffer with 0.1 mM blebbistatin, 0.1 mM E64, 0.5 μM calyculin A, 1× HALT protease inhibitor mixture (Pierce). Samples were prewarmed for 5 min, and assays were initiated with 1 μM calmodulin and 2.5 mM $CaCl_2$ (0.5 mM free Ca^{2+} over 2 mM EGTA). For each measured time, the kinase reaction was terminated with the addition of 100 μl of 20% trichloroacetic acid and 10 mM dithiothreitol. Precipitated proteins were processed using the same method as used for precipitated homogenates for RLC phosphorylation quantification by urea/glycerol-PAGE described above.

Dephosphorylation of RLC in Heart Homogenates and Intact Heart Tissue—For measurement of RLC dephosphorylation in total heart homogenates, WT mouse hearts were snap-frozen in liquid nitrogen within 30 s of excision from anesthetized mice. Frozen hearts were ground in liquid nitrogen, and aliquots were stored at −80 °C. An aliquot of frozen heart powder was immediately homogenized in a 20× volume of chilled homogenization buffer (150 mM NaCl, 50 mM Tris pH 7.4, 1% Nonidet P-40, 1% sodium deoxycholate, 0.1% SDS, 0.2 mM EDTA, 1× HALT protease inhibitor mixture (Pierce)) on ice, and at the indicated times, an aliquot was pipetted into microcentrifuge tubes prefilled with 400 μl of 20% trichloroacetic acid. Precipitated protein samples were then processed for RLC phosphorylation measurements. For measurement of RLC dephosphorylation in intact heart tissue, mice were preinjected with heparin (100 units, intraperitoneally) 10 min prior to anesthesia. Hearts excised from anesthetized mice were immediately rinsed and perfused with a Ca^{2+}-free Tyrode solution by retrograde perfusion through the aorta. At measured times after excision, the ventricle was snap-frozen with clamps that had been prechilled in liquid nitrogen. The frozen heart was then ground in liquid nitrogen and stored at −80 °C. Aliquots of heart powder were precipitated and thawed in 10% trichloroacetic acid and 10 mM dithiothreitol and processed using the same method as used for precipitated total homogenates for RLC phosphorylation measurements.

Isolation of Cardiac Myocytes—Adult mouse cardiac myocytes were isolated by enzymatic digestion of WT mouse hearts using published methods (36) with few modifications. Briefly, mice were preinjected with heparin (100 units, intraperitoneally) 10 min prior to anesthesia. Hearts were immediately rinsed, and blood was removed by retrograde perfusion through the aorta with Krebs-Ringer solution bubbled with 95% CO_2, 5% O_2 (35 mM NaCl, 4.75 mM KCl, 1.19 mM KH_2PO_4, 16 mM Na_2HPO_4, 134 mM sucrose, 10 mM HEPES, 10 mM glucose, 25 mM $NaHCO_3$) at 37 °C. Myocytes were digested free from connective tissues by perfusion of 0.8% collagenase in Krebs-Ringer solution and mechanically separated with forceps and trituration with a disposable transfer pipette in fresh Krebs-Ringer solution. The tissue mixture was then filtered through a metal sieve into a 50-ml conical tube to remove large undigested pieces, and the volume was brought up to 20 ml with fresh Krebs-Ringer solution. Cells were centrifuged at 100 × g for 5 min, and non-muscle cells remaining in suspension were aspirated from the myocyte pellet. The myocyte pellet was washed once more in 10 ml of Krebs-Ringer solution, and cells were collected by centrifugation.

Quantification of cMLCK and MYPT2 in Heart Homogenates—The amount of cMLCK and MYPT2 was determined by quantitative immunoblot analysis using purified proteins as the standard. For cMLCK, a purified GST-tagged fragment containing residues 489–802 was used as the standard. The concentration was determined by a Bradford assay and corrected for its purity as assessed by a Coomassie-stained SDS-

polyacrylamide gel. For MYPT2, recombinant full-length human MYPT2 was used as the standard. The purity of the sample was confirmed by Coomassie staining of proteins separated by SDS-PAGE. Based on previously published values, assumptions made in calculations were that the dry weight of proteins is 20% of tissue weight, the total protein of soluble extract is 10% of wet tissue weight (37), and the density of protein is 1.35 mg/ml (38). The amount of skeletal muscle MLCK in extensor digitorum longus was quantified to confirm measurements with purified rabbit skeletal muscle MLCK used as a standard.

Quantification of MYPT2 Phosphorylation in Ventricles—Endogenous MYPT2 phosphorylation in WT snap-frozen hearts (10 μg) was measured by comparison with a purified protein control (GST-MYPT1(654–880); Millipore, 12-457), which had been phosphorylated to 100% by ROCK1 (Life Technologies, PV3691) using previously published procedures (39). Conservation of MYPT1 residues 654–880 with MYPT2 was confirmed by sequence alignment. Complete phosphorylation was confirmed by immunoblotting for total MYPT1 after separation of non-phosphorylated and phosphorylated forms by 6% Phos-tag-PAGE using routine procedures. Briefly, the resolving gel (10% acrylamide (29:1), 375 mM Tris, pH 8.8, 0.1% SDS, 60 μM $MnCl_2$, 30 μM Phos-tag acrylamide, 0.05% ammonium persulfate, 0.1% TEMED) was overlaid with water-saturated isobutyl alcohol and polymerized for 30 min. Isobutyl alcohol was removed by washing, and standard stacking gel (3.9% acrylamide (29:1), 125 mM Tris, pH 6.8, 0.1% SDS, 0.05% ammonium persulfate, 0.1% TEMED) was polymerized for at least 30 min. ROCK1 assay samples were electrophoresed for ~2 h at 20 mA in 25 mM Tris, 192 mM glycine, and 0.1% SDS until tracking dye migrated out of the gel. The gel was transferred directly onto 0.2-μm pore-sized nitrocellulose membrane (Whatman, Protran) overnight at 0.02 A at room temperature in a modified Phos-tag transfer buffer (25 mM Tris, 192 mM glycine, 0.04% SDS, 10% methanol, and 1 mM EDTA).

Protein Solubility Measurements—Total heart tissue or freshly isolated cardiac myocytes were homogenized and lysed for 20 min on ice in 10 volumes of 50 mM MOPS, pH 7.4, 2 mM EDTA, 2 mM EGTA, 150 mM NaCl, 1 mM DTT, 1% Nonidet P-40, 1× HALT protease inhibitor mixture, 10 μM E64. Aliquots of total homogenate were centrifuged at 100,000 × *g* for 30 min at 4 °C, and supernatant fractions were collected. Equal volumes of total and supernatant fractions were separated by SDS-PAGE and immunoblotted for protein contents.

Adult rat ventricular myocytes were isolated enzymatically from hearts of 200–250-g Sprague-Dawley rats (Harlan Laboratories) according to the method described by Westfall and co-workers (40). Cells were then resuspended in DMEM supplemented with 100 units/ml penicillin and 100 units/ml streptomycin, 5 mM 2,3-butanedione monoxime and plated on laminin-coated (BD Biosciences) chamber slides or glass-bottom culture dishes (MatTeck Corp.). 24 h after incubation, cells were infected with adenovirus expressing GFP-tagged cMLCK at a multiplicity of infection of 10 or 25 for 48 h. Fluorescence images were acquired from live cells before and after permeabilization as described previously (41, 42). Briefly, culture media were removed, and cells were preincubated with 10 mM methyl-β-cyclodextrin for 30 min and then permeabilized with 0.75% Triton X-100 in Ca^{2+}-free PBS for 20 min. Actin was stained by incubating with rhodamine-phalloidin. Cells were kept in a thermal controlled chamber at 37 °C during the course of fluorescence imaging.

RESULTS

Conditional cMLCK Gene Ablation Reduces RLC Phosphorylation in Vivo—A conditional cMLCK knock-out model was generated. Reduction of cMLCK protein in cardiac myocytes of adult mice by 80 ± 2% 2 weeks after the first tamoxifen injection reduced RLC phosphorylation to 0.15 mol of phosphate/mol of RLC (Fig. 1, *A* and *B*). A conventional cMLCK knockout in mice showed that cardiac RLC phosphorylation was reduced to 0.10 mol of phosphate/mol of RLC (Fig. 1, *A* and *B*) (11, 12). The remaining 0.10 mol of phosphate/mol of RLC phosphorylation was confirmed to be serine 15 with tissues from conventional cMLCK knock-out mouse hearts (Fig. 1*C*). The kinase responsible for the residual extent of phosphorylation was not identified. Thus, cMLCK was the primary kinase that phosphorylated RLC *in vivo*, whereas an unidentified protein kinase phosphorylated serine 15 to a small extent. The residual phosphorylation of cardiac RLC with cMLCK knockout is similar to results obtained with skeletal muscle RLC with the knockout of skeletal muscle MLCK (13).

Conditional cMLCK Gene Ablation with Reduced RLC Phosphorylation in Adult Mice Results in Cardiac Dilation—Hearts from conventional cMLCK knock-out mice appeared dilated with a modest increase in heart weight/tibial length compared with hearts from WT mice (11, 12). We explored the possibility that the conventional cMLCK knockout led to an early hypertrophic response, which then progressed to heart failure and dilation. In a conditional knockout of cMLCK induced by tamoxifen injection in adult mice, cMLCK protein decreased with corresponding decreases in RLC phosphorylation by 1 week (Fig. 1). Echocardiographic measurements showed that the decrease in RLC phosphorylation was associated with increased left ventricular internal diameters at diastole and systole and decreased left ventricular fractional shortening, demonstrating a dilated cardiomyopathy phenotype without notable hypertrophy (Fig. 2, *A* and *B*). Tamoxifen-induced decrease in fractional shortening is a known transient phenomenon and did not obscure the RLC phosphorylation-dependent decrease (43). Fibrosis or myofibrillar disarray were also absent, as determined by hematoxylin and eosin (Fig. 2*C*) and trichrome staining (data not shown). Thus, acute reduction of RLC phosphorylation by cMLCK gene ablation was sufficient to impair cardiac performance.

Phosphorylation of TnI and MyBP-C Is Unchanged When RLC Phosphorylation Is Decreased by cMLCK Gene Ablation—Compensatory relationships among TnI, MyBP-C, and RLC phosphorylation were reported for a transgenic model of RLC hypophosphorylation (33). Hence, phosphorylation of regulatory sites on TnI (Ser-23/24) and MyBP-C (Ser-282) were measured in conventional and acute cMLCK gene-ablated animals (Fig. 3, *A* and *B*). Baseline phosphorylation evaluated in the presence of propranolol was included as a control. With propranolol treatment, the extents of MyBP-C and TnI phosphor-

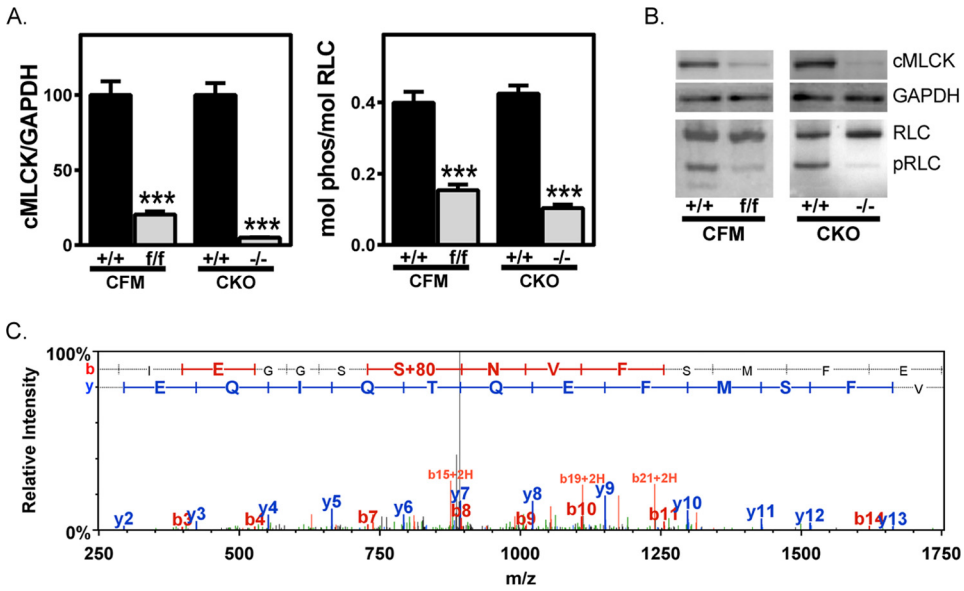

FIGURE 1. **Effect of cMLCK knock-out on cardiac RLC phosphorylation.** The relative quantities of cMLCKs and corresponding cardiac RLC phosphorylation were measured in hearts from CFM (*f/f*) and CKO (−/−) mice. *A*, quantification of kinase (*left*) and corresponding RLC phosphorylation (*right*) relative to respective WT (+/+) control values. Significance was determined by two-tailed unpaired Student's *t* test using GraphPad software; $n \geq 5$; ***, $p < 0.001$, compared with +/+. *B*, representative immunoblot images of measured proteins; grouped from separate images, separated by *white space*. *C*, phosphorylated cardiac RLC from CKO (−/−) mice was subjected to phosphorylation site identification by LC/MS/MS, where 96% of the protein (all residues except for the first seven) was analyzed. The b8 residue that corresponds to serine 15 is the only site phosphorylated. *Error bars*, S.E.

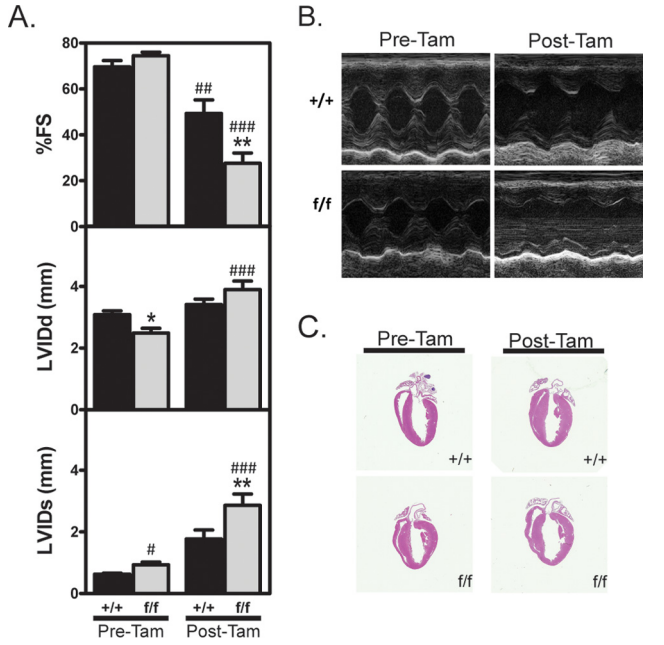

FIGURE 2. **Functional and morphological effects of acute knockout of cMLCK.** *A*, cardiac performance measured by echocardiography in conditional cMLCK gene-ablated (CFM) mice. Comparison of performance pre- and post-tamoxifen (*Tam*) treatment are shown for WT (+/+) and homozygous floxed (*f/f*) mice. Significance was determined by one-way ANOVA, Neuman-Keuls multiple comparison post-test, GraphPad software; $n = 5$; *, $p < 0.05$; **, $p < 0.01$, compared with treatment-matched +/+; #, $p < 0.05$; ##, $p < 0.01$; ###, $p < 0.001$, compared with corresponding pretamoxifen measurements. *B*, representative echocardiography loop images from pre- and post-tamoxifen-injected mice. *C*, representative image of hematoxylin and eosin stain of fixed four-chamber view of 3-month-old male +/+ and f/f, pre- and post-tamoxifen-injected mouse hearts. *Error bars*, S.E.

ylation were decreased in both WT and cMLCK knock-out hearts. Their relative phosphorylation in conditional and conventional cMLCK knock-out mouse hearts was unchanged from WT mice in non-treated (high) and propranolol-treated (low) groups. RLC phosphorylation in hearts from homozygous mice that harbor the TnI R21C mutation that abolishes phosphorylation at the adjacent serines 23/24 (29) was also unchanged from WT in the non-treated and propranolol-treated groups and similar to results obtained with hearts from WT mice (Fig. 3, *C* and *D*).

The Extent of RLC Phosphorylation Is Not Affected by Prolonged β-Adrenergic Stimulation or Inhibition—The results described above showed that β-adrenergic inhibition with propranolol had no effect on RLC phosphorylation while reducing both TnI and MyBP-C phosphorylation. Dobutamine infusion into WT mice was reported to increase cardiac RLC phosphorylation 2-fold compared with basal phosphorylation (33). We evaluated the possibility that cMLCK or other kinases, such as zipper-interacting kinase, may be stimulated to increase RLC phosphorylation *in vivo* with prolonged β-adrenergic stimulation. Whereas dobutamine infusion (5 min) increased the heart rate, and propranolol treatment decreased it (data not shown), RLC phosphorylation remained unaffected (Fig. 4, *A* and *B*). Similar results were obtained with additional dobutamine infusion for 30 min (data not shown). TnI, MyBP-C, and phospholamban phosphorylation were all reduced by propranolol and unaffected by dobutamine treatment. There was no additional increase in TnI phosphorylation with dobutamine infusion over samples from non-treated mice, most likely due to high sympathetic drive under these conditions. Thus, RLC phosphorylation was insensitive to prolonged β-adrenergic stimulation or inhibition.

Phosphorylation of RLC in Native Myosin Filaments and Myofibrils Is a Simple Random Process—Based on the observation that the extent of RLC phosphorylation in normal beating hearts is 0.40 – 0.50 mol of phosphate/mol of RLC, we investi-

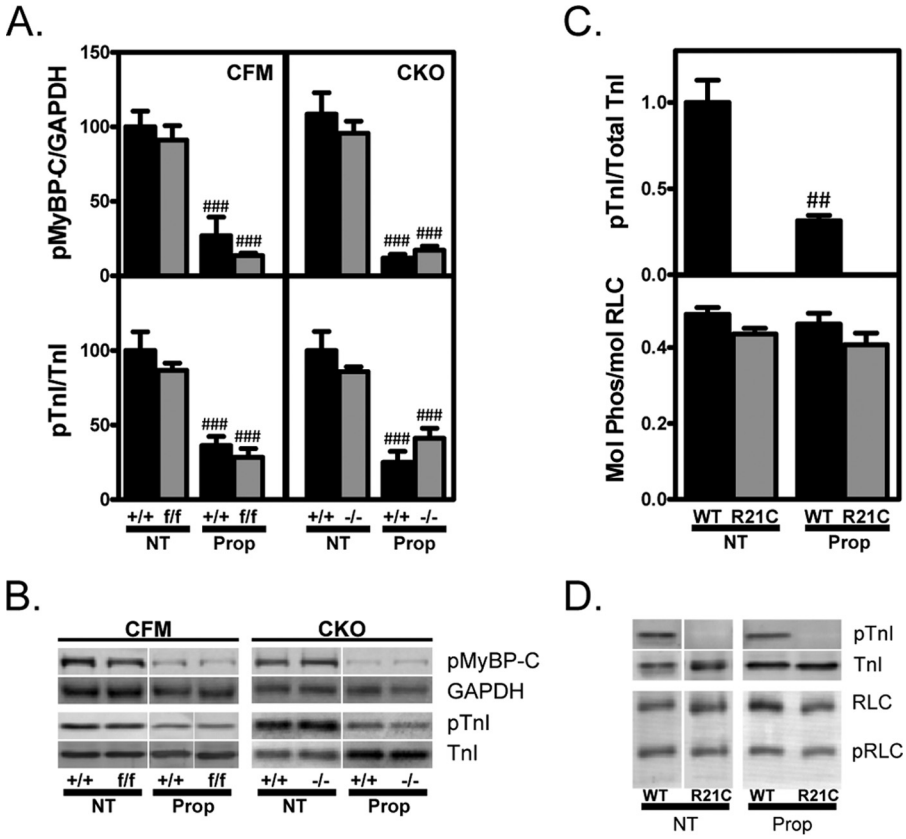

FIGURE 3. **Effects of conditional or conventional knockout of cMLCK on phosphorylation of MyBP-C and TnI.** *A*, phosphorylation measurements of MyBP-C (*top*, *pMyBP-C/GAPDH*), and TnI (*bottom*, *pTnI/total TnI*) in WT (+/+) and respective knockout (*f/f* in CFM and −/− in CKO) mouse hearts that were not treated (*NT*) or treated with propranolol (*Prop*). Percentages relative to average values for controls (+/+) are shown. Significance was determined by one-way ANOVA, Neuman-Keuls multiple comparison post-test, GraphPad software; $n \geq 3$; ###, $p < 0.001$, compared with matched untreated group. *B*, representative immunoblot images of proteins measured in *A*. Images for a given protein grouped by mouse models are from different parts of one immunoblot, separated by *white space*. *C*, quantification of phosphorylation of TnI (*top*, *pTnI/total TnI*), and RLC (*bottom*; *Mol Phos/mol RLC*) in WT and knock-in TnI mutant (R21C) mouse hearts not treated or treated with propranolol. TnI phosphorylation was normalized to the non-treated WT group. There was no detectable TnI phosphorylation in R21C mice. Significance was determined by one-way ANOVA, Neuman-Keuls multiple comparison post-test, GraphPad software; $n \geq 3$; ##, $p < 0.01$, compared with WT, not treated group. *D*, representative immunoblot images of proteins measured in *C*. Images for a given protein grouped by mouse models are from different parts of one immunoblot, separated by *white space*. *Error bars*, S.E.

gated the possibility that one RLC may be more readily phosphorylated than the other in intact myosin. The kinetic properties of RLC phosphorylation in mouse cardiac native myosin filaments dissociated from thin filaments and in mouse cardiac myofibrils were measured (Fig. 5). The concentration of MLCK necessary for complete phosphorylation of RLC by 10 min was determined by kinase titration studies for both substrates (Fig. 5, *inset*). The maximum extents of RLC phosphorylation were 0.87 and 0.97 mol of phosphate/mol of RLC for myofibrils and myosin filaments, respectively. Non-linear regression of the time course of RLC phosphorylation showed a monophasic reaction with no evidence of negative cooperativity (data not shown). Linearization of the reaction, as described previously (44–46), illustrates the monophasic process, indicating that the phosphorylation reaction was kinetically homogeneous (Fig. 5). If half of the RLCs were phosphorylated at a slower rate, the regression would not be monophasic. Thus, phosphorylation of cardiac muscle myosin heads is a simple random process with equal accessibility of both RLCs in each myosin for phosphorylation in both myosin filaments and myofibrils.

RLC Is Maximally Phosphorylated in Intact Paced Trabeculae in the Presence of an MLCP Inhibitor—In order to ascertain whether it was possible to maximally phosphorylate RLC in intact cardiomyocytes, right ventricular trabeculae were paced at increasing frequencies, and RLC phosphorylation was measured (Fig. 6, *A* and *B*). RLC phosphorylation increased to 0.43 ± 0.03 mol of phosphate/mol of RLC in trabeculae paced at 1.5 Hz. In the presence of the MLCP inhibitor calyculin A, RLC phosphorylation increased to 0.91 ± 0.03 mol of phosphate/mol of RLC. Thus, RLC phosphorylation was not inhibited beyond 0.50 mol of phosphate/mol of RLC in intact trabeculae. These results are consistent with the analysis of RLC phosphorylation measured with isolated myosin filaments and myofibrils. Thus, we hypothesized that MLCP activity may limit the extent of RLC phosphorylation in beating hearts.

cMLCK Is Abundant in the Heart—The amount of cMLCK protein in ventricular muscle was determined. A purified fragment of cMLCK (GST-cMLCK(489–802)) was used as a standard, and the amount of cMLCK in heart homogenates was measured by immunoblotting with an antibody raised to the cMLCK sequence (Fig. 7*A*). Calculation of cMLCK in heart tissue using assumptions described under "Experimental Procedures" showed that there was 2.38 ± 0.14 μM cMLCK. The amount of skeletal muscle MLCK in mouse extensor digitorum longus muscle was 0.5 ± 0.03 μM (Fig. 7*B*), consistent with values previously measured for rat white fast twitch skeletal muscle (47).

cMLCK and MLCP Are Distributed Differently in Cardiac Myocytes—In smooth muscles, MYPT1 and smooth muscle MLCK are tightly bound to myosin and actin filaments, respectively, where they participate in phosphorylation and dephosphorylation of smooth muscle RLC (3, 39). Centrifugation of heart homogenates was used to evaluate the relative distributions of cMLCK and MLCP (MYPT2 and PP1cδ) with collection of myofibrils in the pellet fraction. Comparison of total and supernatant fractions of heart homogenates shows that 100 ± 6% of cMLCK was soluble (Fig. 8, *A* and *B*). The solubility of MYPT2 (7.4 ± 2%) and TnI (4.1 ± 2%) was low. Unlike MYPT2, which had low solubility, 61 ± 9% of the catalytic subunit of the myosin phosphatase PP1cδ was soluble (Fig. 8, *A* and *B*). These results demonstrating solubility of cMLCK were confirmed in cardiomyocytes expressing GFP-labeled cMLCK (Fig. 8*C*). Treatment of cells with detergent resulted in the loss of cMLCK-GFP but not myofibrils.

The expression of PP1cδ is not confined to cardiac myocytes but is abundant in smooth and non-muscle cells (48). We therefore measured the relative amount of PP1cδ in ventricular apex tissue containing nonmuscle cells and cardiomyocytes relative to the total lysate and supernatant fraction of isolated cardiomyocytes. The amounts of PP1cδ in the apex and total myocytes were comparable (Fig. 8, *D* and *E*). In isolated myocytes, 62 ± 3% of PP1cδ was soluble (Fig. 8, *D* and *E*). There was very little TnI and RLC in the supernatant fraction from cardiomyo-

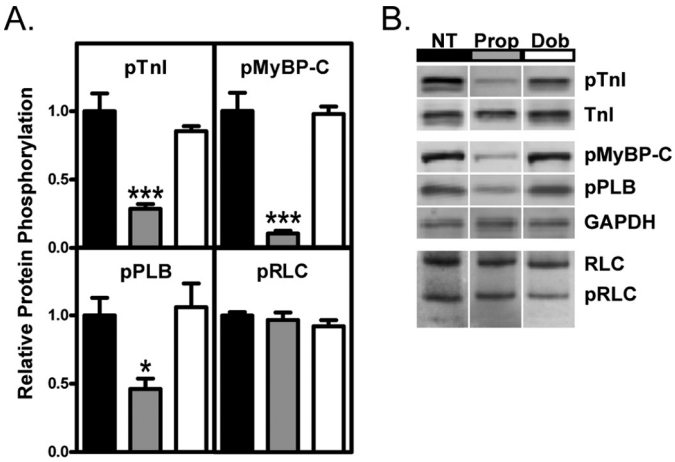

FIGURE 4. **Effects of propranolol and dobutamine on phosphorylation of sarcomeric proteins.** *A*, quantification of phosphorylations of TnI (*pTnI*), MyBP-C (*pMyBP-C*), phospholamban (*pPLB*), and cardiac myosin RLC (*pRLC*), in untreated (*black*), propranolol-treated (*gray*), and dobutamine-treated (*white*) hearts from WT mice. Phosphorylation was normalized to the untreated group. Significance was determined by one-way ANOVA, Neuman-Keuls multiple comparison post-test, GraphPad software; $n \geq 3$; *, $p < 0.05$; ***, $p < 0.001$, compared with not treated. *B*, representative immunoblot images of proteins measured. Treatments are as indicated: not treated (*NT*), propranolol-treated (*Prop*), and dobutamine-treated (*Dob*). Images for a given protein grouped by treatment are from different parts of one immunoblot, separated by *white space*. *Error bars*, S.E.

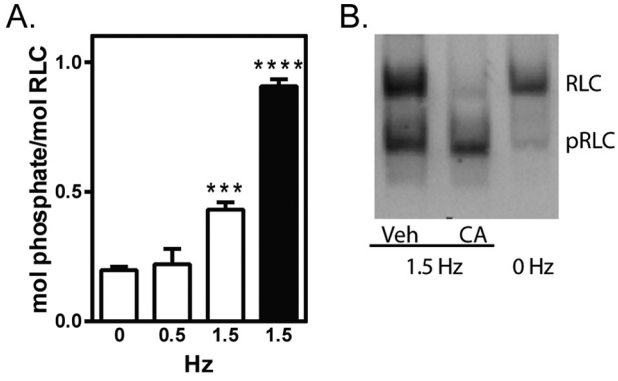

FIGURE 6. **RLC phosphorylation in paced ventricular trabeculae.** *A*, quantification of RLC phosphorylation in mouse right ventricular trabeculae in response to 30 min of electrical stimulation (0–1.5 Hz) in the absence (*white bars*) and presence (*black bar*) of 1 μM calyculin A (*CA*). *B*, representative immunoblot image. Significance was determined by one-way ANOVA, Neuman-Keuls multiple comparison post-test, GraphPad software; $n \geq 3$; ***, $p <$ 0.001, compared with unpaced trabeculae (0 Hz). *Error bars*, S.E.

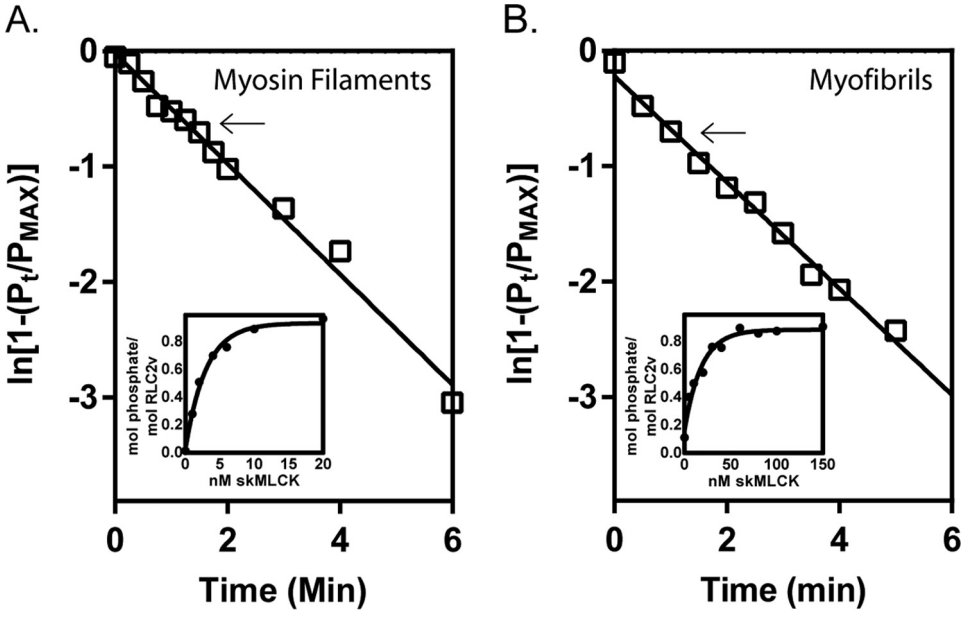

FIGURE 5. **Representative time course of phosphorylation of RLC in intact native mouse cardiac myosin filaments (*A*) and mouse cardiac myofibrils (*B*) by purified rabbit skeletal muscle MLCK.** Reactions were initiated by the addition of Ca^{2+}/calmodulin at $t = 0$; P_t, mol of phosphate/mol of RLC measured at time t; P_{MAX}, maximum phosphorylation of RLC. *Inset*, complete saturating profile of RLC phosphorylation for increasing concentrations of MLCK with 0–20 nM for myosin filaments or 0–150 nM for myofibrils measured at 10 min. *Arrows*, RLC phosphorylation at 0.5 mol of phosphate/mol of RLC.

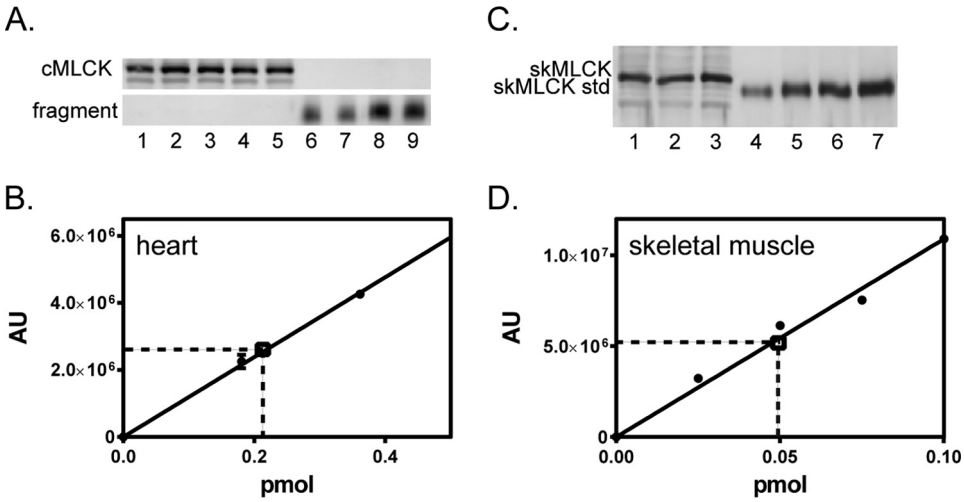

FIGURE 7. **Quantification of MLCKs in cardiac ventricular and fast twitch skeletal muscle.** *A*, immunoblot of cardiac MLCK in 10 μg of total protein from WT mouse ventricles (*lanes 1–5*) compared with purified cMLCK protein standard (*lanes 6–9*). *B*, cMLCK immunoblot signal intensity in arbitrary units (*AU*) plotted against pmol of protein standard. *C*, immunoblot of skeletal MLCK (*skMLCK*) in 10 μg of total protein from WT mouse extensor digitorum longus (*lanes 1–3*) compared with purified rabbit skeletal MLCK protein standard (*lanes 4–7*). *D*, skeletal MLCK immunoblot signal intensity in arbitrary units (*AU*) plotted against pmol of protein standard.

cytes, whereas cMLCK was abundant (Fig. 8, *D* and *E*). Thus, there are differential distributions of soluble cMLCK and MYPT2-regulated MLCP associated with myofibrils containing TnI and RLC.

MYPT2 Is Abundant and Phosphorylated in Ventricular Heart Tissue—Because cMLCK protein is abundant in ventricular muscle, we measured the total amount of MYPT2 protein and phosphorylation at its inhibitory site, threonine 646. A fragment of MYPT1 (residues 654–880) containing the same phosphorylation site was phosphorylated by ROCK1 as a control to quantify the amount of MYPT2 phosphorylation. MYPT1 and the fragment have two sites phosphorylated by ROCK1, one of which is also contained in MYPT2. Complete diphosphorylation of the fragment was confirmed by maximal ^{32}P incorporation over time (data not shown) and an immunoblot of proteins separated by Phos-tag gel (Fig. 9*A*). The ratio of phosphorylated MYPT2 to total MYPT2 in the heart was calculated by normalizing the immunoblot measurements to the control. In normal WT mice, 100 ± 7% (n = 6) of MYPT2 was phosphorylated (Fig. 9, *B* and *C*). The amount of MYPT2 in total heart homogenates was estimated to be 11 ± 1.2 μM (n = 5) by comparison with purified full-length human MYPT2 (Fig. 9, *D* and *E*). Thus, there was about 5-fold more MYPT2 than cMLCK. Importantly, MYPT2 was maximally phosphorylated at threonine 646 in beating hearts.

RLC Dephosphorylation Is Slow in Cardiac Tissues but Not in Homogenates—The rate of RLC dephosphorylation was measured in intact non-beating hearts and homogenates. RLC and MYPT2 in intact non-beating hearts perfused with Ca^{2+}-free Tyrode solution were not significantly dephosphorylated within 20 min (Fig. 10, *A* and *B*), but RLC phosphorylation was reduced to 0.26 ± 0.02 mol of phosphate/mol after 60 min and 0.06 ± 0.02 mol of phosphate/mol after 2 h of perfusion. MYPT2 phosphorylation was reduced to 61 ± 7% after 60 min and 23 ± 8% after 2 h of perfusion. The residual RLC phosphorylation which remains in cMLCK knock-out hearts was also not significantly reduced within 20 min of heart excision (Fig. 10, *A* and *B*). Freshly isolated cardiomyocytes from nonbeating hearts have 0.06 ± 0.02 mol of phosphate/mol of RLC phosphorylation (n = 3). In contrast to results obtained with perfused hearts, both RLC and MYPT2 were rapidly dephosphorylated in homogenates in the absence but not in the presence of calyculin A (Fig. 10, *A* and *C*). In the absence of calyculin A, RLC phosphorylation was reduced to 0.12 ± 0.02 mol of phosphate/mol, and MYPT2 phosphorylation was reduced to 1.8 ± 0.4% in homogenates after 20 min. Thus, the normal beating of the heart required for RLC phosphorylation is consistent with Ca^{2+}/calmodulin-dependent phosphorylation by cMLCK. The signaling mechanisms for phosphorylation of the abundant MYPT2 are not clear, but its high phosphorylation is similar to the constitutive phosphorylation of MYPT1 in smooth muscle (39).

DISCUSSION

Inotropic responses to adrenergic stimulation are mediated in part by phosphorylations of MyBP-C and TnI, resulting in modulation of actomyosin activity. The effects of phosphorylations of these proteins on actomyosin activity have been measured in various systems and under conditions where only a specific protein was phosphorylated (49–55). Phosphorylation of MyBP-C accelerates the rate of actomyosin interaction, and phosphorylation of TnI increases the rate of relaxation (49–53). RLC phosphorylation changes myosin cross-bridge properties, increasing the Ca^{2+} sensitivity and accelerating rates of actomyosin interaction (54, 55). Considering these functional interactions of spatially close sarcomeric proteins, we used conventional and conditional cMLCK knock-out mouse models to test whether compensatory phosphorylation of TnI or MyBP-C occurs to enhance cardiac function when RLC phosphorylation is acutely or chronically reduced. There were no significant changes in TnI or MyBP-C phosphorylation in mice with acute or chronic attenuation of RLC phosphorylation. Consistent with a lack of influence of RLC phosphorylation on TnI phosphorylation, TnI dephosphorylation resulting from propranolol treatment or the lack of TnI phosphorylation in knock-

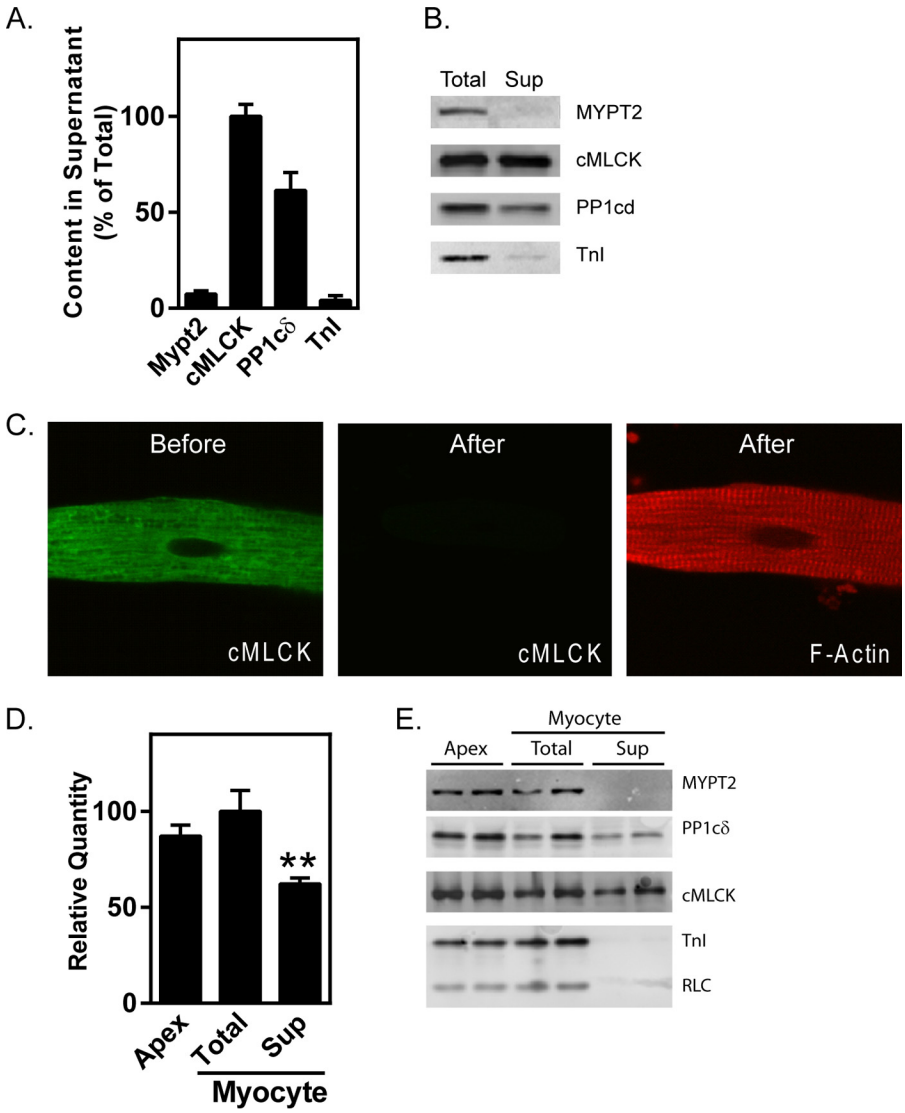

FIGURE 8. **Distribution of cMLCK and MLCP subunits in cardiac homogenates.** *A*, relative distribution of proteins in supernatant (*sup*) fractions after centrifugation at 100,000 × *g* for 30 min at 4 °C; average of $n \geq 4$. *B*, representative immunoblot of proteins measured in *A*. *C*, representative image of association of GFP-cMLCK with myofilament proteins in non-fixed adult rat ventricular myocyte imaged before and after live cell permeabilization. Actin filaments imaged with rhodamine-phalloidin after permeabilization. *D*, comparison of PP1cδ protein content in total proteins of the apex of the mouse heart and isolated cardiomyocyte lysates separated by centrifugation at 100,000 × *g* for 30 min at 4 °C. Significance between myocyte total and supernatant fractions was determined by Student's *t* test, GraphPad software; $n = 3$; **, $p < 0.01$. *E*, representative immunoblot of PP1cδ protein measured in *C*. MYPT2, cMLCK, TnI, and RLC are shown as controls for protein separation by centrifugation. *Error bars*, S.E.

in mice containing the TnI R21C mutation did not affect RLC phosphorylation. Furthermore, the dephosphorylation of MyBP-C and phospholamban induced by propranolol treatment did not affect the level of RLC phosphorylation. A decrease in TnI phosphorylation was reported in transgenic mice overexpressing nonphosphorylatable RLC (33), but based on the lack of similar effects in our cMLCK knock-out mice, the reported effect may be specific to the transgenic mouse line or due to desensitization effects known to occur with chronic heart failure (56, 57). Thus, the constitutive basal phosphorylation of RLC in beating hearts appears not to be influenced by the phosphorylation of other thick or thin filament proteins and represents a balance between slow phosphorylation and dephosphorylation rates (22–24).

Consistent with previous reports, we found that RLC phosphorylation was not sensitive to acute β-adrenergic stimulation or inhibition (25–27). In addition, the high sympathetic tone in these mice prevented dobutamine infusions from further increasing TnI, MyBP-C, or phospholamban phosphorylation, consistent with findings by Scruggs *et al.* (33) and Wang *et al.* (30). Our RLC phosphorylation measurements, however, differ from the finding of Scruggs *et al.* (33) that dobutamine infusion increased RLC phosphorylation in WT mice (33). We did not find an increase with infusion for 5 or 30 min or with a higher dobutamine dose of 32 ng/g/min (data not shown). Processing procedures for RLC phosphorylation measurements may account for the different results. Our snap-frozen heart samples are fixed directly into trichloroacetic acid to denature all proteins, including protein phosphatases and proteases. Without the acid precipitation step, RLC may be dephosphorylated in heart homogenates without sufficient chemical phosphatase inhibitors (23). Indeed, our results show that RLC is rapidly

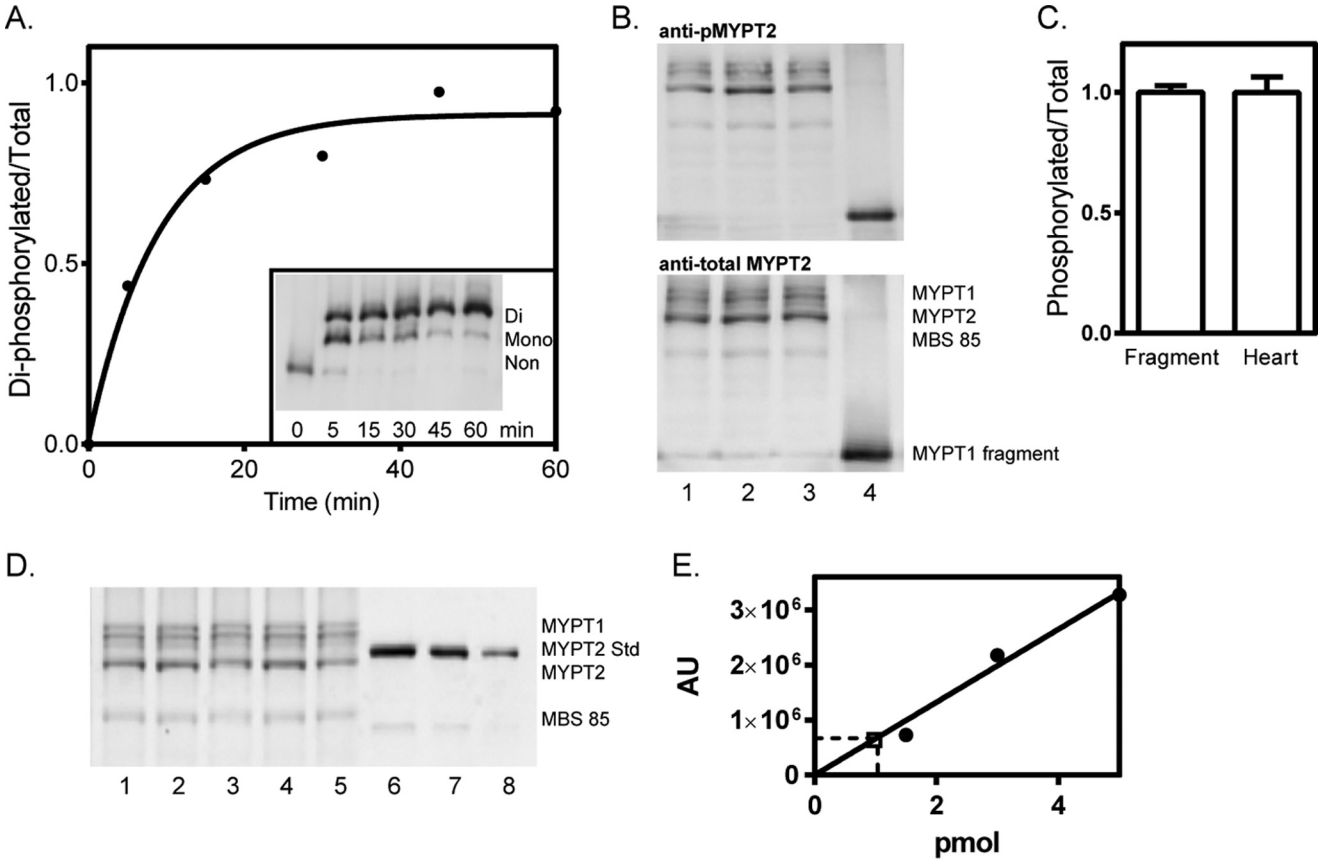

FIGURE 9. **Measurement of MYPT2 amount and phosphorylation in mouse ventricles.** *A*, time course of maximal phosphorylation of an MYPT2 standard (purified GST-MYPT1 fragment, residues 654–880) by ROCK1. *Inset*, immunoblot of the phosphorylated standard separated by Phos-tag gel. *B*, representative immunoblot images comparing phosphorylated MYPT2 and total MYPT2 in total mouse heart homogenates (*lanes 1–3*) against the signal from the fully phosphorylated MYPT1 fragment standard (*lane 4*), using antibodies targeted to phosphorylated MYPT2 (*pMYPT2*) and total MYPT2. *C*, ratio of phosphorylated MYPT2 in heart homogenates, normalized to mean GST-MYPT1 fragment ($n = 6$). *D*, representative immunoblot of MYPT2 protein in 10 μg of total mouse heart homogenates (*lanes 1–5*) compared with purified human MYPT2 protein standard control (*lanes 6–8*). *E*, MYPT2 immunoblot signal intensity in arbitrary units (*AU*) plotted against pmol of protein standard. *Error bars*, S.E.

dephosphorylated in heart homogenates without a chemical inhibitor, such as calyculin A. Ice-chilled tissues in Scruggs *et al.* (33) were homogenized in a nondenaturing aqueous buffer containing an unspecified amount of a mixture of protein phosphatase inhibitors, and then myofilaments were processed through several steps before dissolving proteins in Laemmli buffer. Based on their published representative blot, a possible explanation is that some of their control samples became dephosphorylated. Their assessment of RLC phosphorylation with dobutamine infusion was performed by relative changes with a phosphospecific cardiac RLC antibody rather than quantitative measurements, such as isoelectric focusing or urea/glycerol PAGE (33).

Given the difficulty in increasing RLC phosphorylation with β-adrenergic stimulation, we considered the possibility that RLC phosphorylation in intact ventricular myosins was limited to 40–50% by intra- or intermolecular steric constraints. Asymmetric head to head interaction within the cardiac myosin dimer in the ATP-bound relaxed state was revealed by cryo-electron microscopy in native myosin filaments (35). Intramolecular block of one myosin head by another might sterically constrain one RLC if the position of the blocked myosin head compromised the accessibility of the RLC phosphorylation site. Measurements of the position of MyBP-C by electron micrograph of the cardiac sarcomere have shown that it binds to every third myosin crown (4), and binding of MyBP-C to RLC (58) has also been proposed. In addition, binding of actin by the essential light chain on myosin has been proposed (59), which would bring RLC closer to the thin filament. Thus, we hypothesized that within the myofibrils, intramolecular and/or intermolecular steric constraints could limit the accessibility of RLC for phosphorylation. However, our biochemical analyses with myosin filaments or myofibrils did not support this hypothesis. RLC phosphorylation occurred via a single pseudo-first order process in both intact myosin filaments and myofibrillar preparations. Lack of a biphasic rate rules out intramolecular block of one RLC by another and confirms that phosphorylation of the two RLCs is a stochastic process. These results were further supported by 91% monophosphorylation of intact right ventricular trabeculae in the presence of a cell-permeant chemical inhibitor of MLCP. Although diphosphorylation of RLC was reported in a rodent disease model (60), we did not see significant diphosphorylation of RLC in mouse myosin filaments or myofibrils even with prolonged incubation with high concentrations of skeletal MLCK. Thus, kinetic properties of phosphorylation of cardiac RLC bound to myosin heavy chain suggest a random process, similar to results reported for skeletal (46) and smooth muscle (61) myosins.

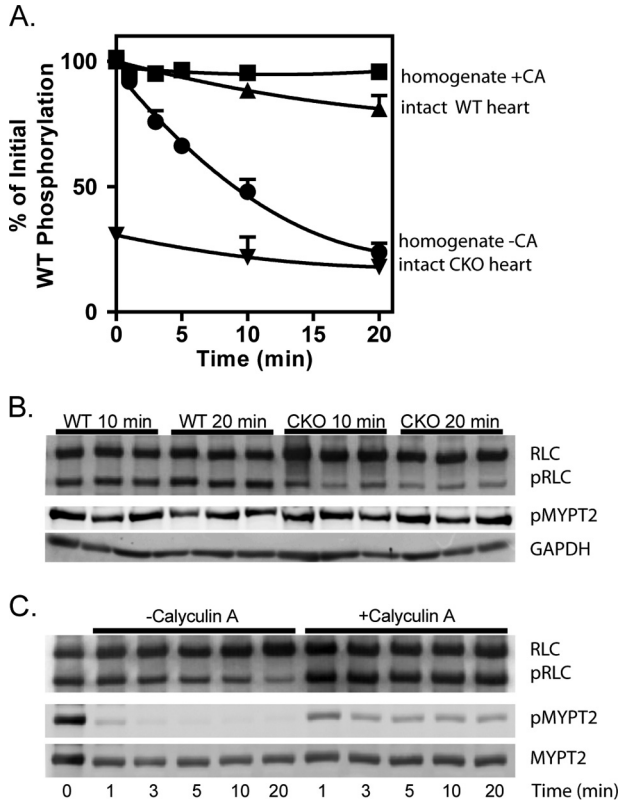

FIGURE 10. **Comparison of RLC dephosphorylation in heart homogenates and intact hearts.** *A*, time course of RLC dephosphorylation represented as a percentage of WT RLC phosphorylation, measured by immunoblot of RLCs separated by glycerol/PAGE. *Squares*, total WT heart homogenate with 1 μM calyculin A; *upright triangles*, intact WT heart perfused with Ca^{2+}-free Tyrode solution; *circles*, total WT heart homogenate without added phosphatase inhibitors; *inverted triangles*, intact cMLCK heart perfused with Ca^{2+}-free Tyrode solution. Average of $n = 3$; some error bars are obscured by *symbols*. *B*, representative immunoblot of RLCs in intact WT or CKO mice hearts, dephosphorylated for 10 or 20 min. *C*, representative immunoblots of proteins in WT total heart homogenates, dephosphorylated for 1–20 min. Matched samples are shown. *Error bars*, S.E.

The extent of RLC phosphorylation in different tissues and cells is determined by the balance of kinase and phosphatase activities. RLC was dephosphorylated in non-beating hearts, similar to results obtained in rat (23) and rabbit (24) hearts. We also noted that RLC was dephosphorylated in isolated adult cardiac myocytes. The simplest interpretation is that the reduction in $[Ca^{2+}]_i$ transients inhibits cMLCK, as observed for RLC phosphorylation in skeletal muscle by Ca^{2+}/calmodulin-dependent MLCK (47, 62). However, additional biochemical investigation is needed to resolve the conflicting reports (17, 18) about Ca^{2+}/calmodulin dependence of cMLCK.

MLCP activity is regulated in different tissues and cells (48). In smooth muscle, MYPT1 is constitutively phosphorylated, and MYPT1 phosphorylation reduces but does not eliminate MLCP activity (39). In the absence of MYPT1, smooth muscle RLC was still dephosphorylated by PP1cδ during relaxation, indicating that soluble PP1cδ not bound to MYPT1 is still active toward phosphorylated smooth muscle RLC (39). The constitutive phosphorylation of MYPT1 was presumably due to ROCK and other unidentified protein kinases. MYPT2 was also constitutively phosphorylated in the heart, implying inhibition of MLCP activity. This observation is consistent with slow dephosphorylation of RLC and MYPT2 in intact tissues. However, the high extent of RLC phosphorylation in paced trabeculae in the presence of calyculin A suggests a significant contribution of MLCP activity to basal RLC phosphorylation in beating hearts. Similar to results reported on the solubility of PP1cδ in smooth muscle (39), a large fraction of PP1cδ in the cardiomyocytes was soluble and not bound to the MLCP regulatory subunit MYPT2 that targets PP1cδ to myosin filaments. Thus, a fraction of PP1cδ not regulated by MYPT2 may contribute to MLCP phosphatase activity toward RLC in the heart. The protein kinase that constitutively phosphorylates MYPT2 and the determination of different forms of PP1c that may dephosphorylate myosin require additional investigation.

In summary, the constitutive phosphorylation of RLC in beating hearts may be due to the combined activities of Ca^{2+}/calmodulin-dependent cMLCK in equilibrium with the MLCP activity. Although cMLCK is abundantly expressed in cardiac muscle, its specific activity is low, which is consistent with the slow turnover rate ($t_{1/2} = 90$ min) of phosphate in RLC in beating hearts (23) as well as the slow rephosphorylation of RLC when noncontracting heart muscle is paced (24). At low, but not high, frequencies of stimulation, the extent of RLC phosphorylation is proportional to the frequency of stimulation (24). These frequency dependence observations are similar to results reported for skeletal muscle (13) and imply that in mouse heart beating at a high frequency, cMLCK may be maximally activated by Ca^{2+}/calmodulin, although its activity is low.

Acknowledgments—We are indebted to Masumi Eto for purified MYPT1 fragment, Masaaki Ito for purified MYPT2, Herwig Schuler for cMLCK, Kathy Trybus for purified skeletal muscle MLCK, and Maria Zhogbi and Roger Craig for the detailed protocol for preparation of native mouse cardiac myosin filaments.

REFERENCES

1. Geeves, M. A., and Holmes, K. C. (2005) The molecular mechanism of muscle contraction. *Adv. Protein Chem.* **71,** 161–193
2. Solaro, R. J. (2010) Sarcomere control mechanisms and the dynamics of the cardiac cycle. *J. Biomed. Biotechnol.* **2010,** 105648
3. Kamm, K. E., and Stull, J. T. (2011) Signaling to myosin regulatory light chain in sarcomeres. *J. Biol. Chem.* **286,** 9941–9947
4. Moss, R. L., Fitzsimons, D. P., and Ralphe, J. C. (2015) Cardiac MyBP-C regulates the rate and force of contraction in mammalian myocardium. *Circ. Res.* **116,** 183–192
5. Sheikh, F., Lyon, R. C., and Chen, J. (2014) Getting the skinny on thick filament regulation in cardiac muscle biology and disease. *Trends Cardiovasc. Med.* **24,** 133–141
6. Kuster, D. W., Bawazeer, A. C., Zaremba, R., Goebel, M., Boontje, N. M., and van der Velden, J. (2012) Cardiac myosin binding protein C phosphorylation in cardiac disease. *J. Muscle Res. Cell Motil.* **33,** 43–52
7. McNally, E. M., Golbus, J. R., and Puckelwartz, M. J. (2013) Genetic mutations and mechanisms in dilated cardiomyopathy. *J. Clin. Invest.* **123,** 19–26
8. Sanbe, A., Fewell, J. G., Gulick, J., Osinska, H., Lorenz, J., Hall, D. G., Murray, L. A., Kimball, T. R., Witt, S. A., and Robbins, J. (1999) Abnormal cardiac structure and function in mice expressing nonphosphorylatable cardiac regulatory myosin light chain 2. *J. Biol. Chem.* **274,** 21085–21094
9. Sheikh, F., Ouyang, K., Campbell, S. G., Lyon, R. C., Chuang, J., Fitzsimons, D., Tangney, J., Hidalgo, C. G., Chung, C. S., Cheng, H., Dalton, N. D., Gu, Y., Kasahara, H., Ghassemian, M., Omens, J. H., Peterson, K. L., Granzier, H. L., Moss, R. L., McCulloch, A. D., and Chen, J. (2012) Mouse and

computational models link Mlc2v dephosphorylation to altered myosin kinetics in early cardiac disease. *J. Clin. Invest.* **122,** 1209–1221
10. Chang, A. N., Chen, G., Gerard, R. D., Kamm, K. E., and Stull, J. T. (2010) Cardiac myosin is a substrate for zipper-interacting protein kinase (ZIPK). *J. Biol. Chem.* **285,** 5122–5126
11. Chang, A. N., Huang, J., Battiprolu, P. K., Hill, J. A., Kamm, K. E., and Stull, J. T. (2013) The effects of neuregulin on cardiac Myosin light chain kinase gene-ablated hearts. *PLoS One* **8,** e66720
12. Ding, P., Huang, J., Battiprolu, P. K., Hill, J. A., Kamm, K. E., and Stull, J. T. (2010) Cardiac myosin light chain kinase is necessary for myosin regulatory light chain phosphorylation and cardiac performance *in vivo*. *J. Biol. Chem.* **285,** 40819–40829
13. Zhi, G., Ryder, J. W., Huang, J., Ding, P., Chen, Y., Zhao, Y., Kamm, K. E., and Stull, J. T. (2005) Myosin light chain kinase and myosin phosphorylation effect frequency-dependent potentiation of skeletal muscle contraction. *Proc. Natl. Acad. Sci. U.S.A.* **102,** 17519–17524
14. Kamm, K. E., and Stull, J. T. (2001) Dedicated myosin light chain kinases with diverse cellular functions. *J. Biol. Chem.* **276,** 4527–4530
15. Huang, J., Shelton, J. M., Richardson, J. A., Kamm, K. E., and Stull, J. T. (2008) Myosin regulatory light chain phosphorylation attenuates cardiac hypertrophy. *J. Biol. Chem.* **283,** 19748–19756
16. Warren, S. A., Briggs, L. E., Zeng, H., Chuang, J., Chang, E. I., Terada, R., Li, M., Swanson, M. S., Lecker, S. H., Willis, M. S., Spinale, F. G., Maupin-Furlowe, J., McMullen, J. R., Moss, R. L., and Kasahara, H. (2012) Myosin light chain phosphorylation is critical for adaptation to cardiac stress. *Circulation* **126,** 2575–2588
17. Chan, J. Y., Takeda, M., Briggs, L. E., Graham, M. L., Lu, J. T., Horikoshi, N., Weinberg, E. O., Aoki, H., Sato, N., Chien, K. R., and Kasahara, H. (2008) Identification of cardiac-specific myosin light chain kinase. *Circ. Res.* **102,** 571–580
18. Seguchi, O., Takashima, S., Yamazaki, S., Asakura, M., Asano, Y., Shintani, Y., Wakeno, M., Minamino, T., Kondo, H., Furukawa, H., Nakamaru, K., Naito, A., Takahashi, T., Ohtsuka, T., Kawakami, K., Isomura, T., Kitamura, S., Tomoike, H., Mochizuki, N., and Kitakaze, M. (2007) A cardiac myosin light chain kinase regulates sarcomere assembly in the vertebrate heart. *J. Clin. Invest.* **117,** 2812–2824
19. Moorhead, G., Johnson, D., Morrice, N., and Cohen, P. (1998) The major myosin phosphatase in skeletal muscle is a complex between the β-isoform of protein phosphatase 1 and the MYPT2 gene product. *FEBS Lett.* **438,** 141–144
20. Okamoto, R., Kato, T., Mizoguchi, A., Takahashi, N., Nakakuki, T., Mizutani, H., Isaka, N., Imanaka-Yoshida, K., Kaibuchi, K., Lu, Z., Mabuchi, K., Tao, T., Hartshorne, D. J., Nakano, T., and Ito, M. (2006) Characterization and function of MYPT2, a target subunit of myosin phosphatase in heart. *Cell. Signal.* **18,** 1408–1416
21. Mizutani, H., Okamoto, R., Moriki, N., Konishi, K., Taniguchi, M., Fujita, S., Dohi, K., Onishi, K., Suzuki, N., Satoh, S., Makino, N., Itoh, T., Hartshorne, D. J., and Ito, M. (2010) Overexpression of myosin phosphatase reduces Ca^{2+} sensitivity of contraction and impairs cardiac function. *Circ. J.* **74,** 120–128
22. Herring, B. P., and England, P. J. (1986) The turnover of phosphate bound to myosin light chain-2 in perfused rat heart. *Biochem. J.* **240,** 205–214
23. High, C. W., and Stull, J. T. (1980) Phosphorylation of myosin in perfused rabbit and rat hearts. *Am. J. Physiol.* **239,** H756–H764
24. Silver, P. J., Buja, L. M., and Stull, J. T. (1986) Frequency-dependent myosin light chain phosphorylation in isolated myocardium. *J. Mol. Cell Cardiol.* **18,** 31–37
25. Dias, F. A., Walker, L. A., Arteaga, G. M., Walker, J. S., Vijayan, K., Peña, J. R., Ke, Y., Fogaca, R. T., Sanbe, A., Robbins, J., and Wolska, B. M. (2006) The effect of myosin regulatory light chain phosphorylation on the frequency-dependent regulation of cardiac function. *J. Mol. Cell Cardiol.* **41,** 330–339
26. Grimm, M., Haas, P., Willipinski-Stapelfeldt, B., Zimmermann, W. H., Rau, T., Pantel, K., Weyand, M., and Eschenhagen, T. (2005) Key role of myosin light chain (MLC) kinase-mediated MLC2a phosphorylation in the α1-adrenergic positive inotropic effect in human atrium. *Cardiovasc. Res.* **65,** 211–220
27. Jeacocke, S. A., and England, P. J. (1980) Phosphorylation of myosin light chains in perfused rat heart: effect of adrenaline and increased cytoplasmic calcium ions. *Biochem. J.* **188,** 763–768
28. Sakai, K., and Miyazaki, J. (1997) A transgenic mouse line that retains Cre recombinase activity in mature oocytes irrespective of the cre transgene transmission. *Biochem. Biophys. Res. Commun.* **237,** 318–324
29. Dweck, D., Sanchez-Gonzalez, M. A., Chang, A. N., Dulce, R. A., Badger, C. D., Koutnik, A. P., Ruiz, E. L., Griffin, B., Liang, J., Kabbaj, M., Fincham, F. D., Hare, J. M., Overton, J. M., and Pinto, J. R. (2014) Long term ablation of protein kinase A (PKA)-mediated cardiac troponin I phosphorylation leads to excitation-contraction uncoupling and diastolic dysfunction in a knock-in mouse model of hypertrophic cardiomyopathy. *J. Biol. Chem.* **289,** 23097–23111
30. Wang, Y., Pinto, J. R., Solis, R. S., Dweck, D., Liang, J., Diaz-Perez, Z., Ge, Y., Walker, J. W., and Potter, J. D. (2012) Generation and functional characterization of knock-in mice harboring the cardiac troponin I-R21C mutation associated with hypertrophic cardiomyopathy. *J. Biol. Chem.* **287,** 2156–2167
31. Collins, K. A., Korcarz, C. E., Shroff, S. G., Bednarz, J. E., Fentzke, R. C., Lin, H., Leiden, J. M., and Lang, R. M. (2001) Accuracy of echocardiographic estimates of left ventricular mass in mice. *Am. J. Physiol. Heart Circ. Physiol.* **280,** H1954–H1962
32. Kamm, K. E., Hsu, L. C., Kubota, Y., and Stull, J. T. (1989) Phosphorylation of smooth muscle myosin heavy and light chains: effects of phorbol dibutyrate and agonists. *J. Biol. Chem.* **264,** 21223–21229
33. Scruggs, S. B., Hinken, A. C., Thawornkaiwong, A., Robbins, J., Walker, L. A., de Tombe, P. P., Geenen, D. L., Buttrick, P. M., and Solaro, R. J. (2009) Ablation of ventricular myosin regulatory light chain phosphorylation in mice causes cardiac dysfunction *in situ* and affects neighboring myofilament protein phosphorylation. *J. Biol. Chem.* **284,** 5097–5106
34. Solaro, R. J., Pang, D. C., and Briggs, F. N. (1971) The purification of cardiac myofibrils with Triton X-100. *Biochim. Biophys. Acta* **245,** 259–262
35. Zoghbi, M. E., Woodhead, J. L., Moss, R. L., and Craig, R. (2008) Three-dimensional structure of vertebrate cardiac muscle myosin filaments. *Proc. Natl. Acad. Sci. U.S.A.* **105,** 2386–2390
36. O'Connell, T. D., Rodrigo, M. C., and Simpson, P. C. (2007) Isolation and culture of adult mouse cardiac myocytes. *Methods Mol. Biol.* **357,** 271–296
37. Benson, E. S. (1955) Composition and state of protein in heart muscle of normal dogs and dogs with experimental myocardial failure. *Circ. Res.* **3,** 221–228
38. Fischer, H., Polikarpov, I., and Craievich, A. F. (2004) Average protein density is a molecular-weight-dependent function. *Protein Sci.* **13,** 2825–2828
39. Tsai, M. H., Chang, A. N., Huang, J., He, W., Sweeney, H. L., Zhu, M., Kamm, K. E., and Stull, J. T. (2014) Constitutive phosphorylation of myosin phosphatase targeting subunit-1 in smooth muscle. *J. Physiol.* **592,** 3031–3051
40. Metzger, J. M., Samuelson, L. C., Rust, E. M., and Westfall, M. V. (1997) Embryonic stem cell cardiogenesis applications for cardiovascular research. *Trends Cardiovasc. Med.* **7,** 63–68
41. Lin, P., Luby-Phelps, K., and Stull, J. T. (1997) Binding of myosin light chain kinase to cellular actin-myosin filaments. *J. Biol. Chem.* **272,** 7412–7420
42. Lin, P., Luby-Phelps, K., and Stull, J. T. (1999) Properties of filament-bound myosin light chain kinase. *J. Biol. Chem.* **274,** 5987–5994
43. Koitabashi, N., Bedja, D., Zaiman, A. L., Pinto, Y. M., Zhang, M., Gabrielson, K. L., Takimoto, E., and Kass, D. A. (2009) Avoidance of transient cardiomyopathy in cardiomyocyte-targeted tamoxifen-induced MerCreMer gene deletion models. *Circ. Res.* **105,** 12–15
44. Orsi, B. A., and Tipton, K. F. (1979) Kinetic analysis of progress curves. *Methods Enzymol.* **63,** 159–183
45. Persechini, A., and Hartshorne, D. J. (1983) Ordered phosphorylation of the two 20,000 molecular weight light chains of smooth muscle myosin. *Biochemistry* **22,** 470–476
46. Persechini, A., and Stull, J. T. (1984) Phosphorylation kinetics of skeletal muscle myosin and the effect of phosphorylation on actomyosin adenosinetriphosphatase activity. *Biochemistry* **23,** 4144–4150

47. Moore, R. L., and Stull, J. T. (1984) Myosin light chain phosphorylation in fast and slow skeletal muscles *in situ*. *Am. J. Physiol.* **247,** C462–C471
48. Matsumura, F., and Hartshorne, D. J. (2008) Myosin phosphatase target subunit: many roles in cell function. *Biochem. Biophys. Res. Commun.* **369,** 149–156
49. Colson, B. A., Rybakova, I. N., Prochniewicz, E., Moss, R. L., and Thomas, D. D. (2012) Cardiac myosin binding protein-C restricts intrafilament torsional dynamics of actin in a phosphorylation-dependent manner. *Proc. Natl. Acad. Sci. U.S.A.* **109,** 20437–20442
50. Stelzer, J. E., Patel, J. R., Walker, J. W., and Moss, R. L. (2007) Differential roles of cardiac myosin-binding protein C and cardiac troponin I in the myofibrillar force responses to protein kinase A phosphorylation. *Circ. Res.* **101,** 503–511
51. Weisberg, A., and Winegrad, S. (1996) Alteration of myosin cross bridges by phosphorylation of myosin-binding protein C in cardiac muscle. *Proc. Natl. Acad. Sci. U.S.A.* **93,** 8999–9003
52. Kentish, J. C., McCloskey, D. T., Layland, J., Palmer, S., Leiden, J. M., Martin, A. F., and Solaro, R. J. (2001) Phosphorylation of troponin I by protein kinase A accelerates relaxation and crossbridge cycle kinetics in mouse ventricular muscle. *Circ. Res.* **88,** 1059–1065
53. Zhang, R., Zhao, J., Mandveno, A., and Potter, J. D. (1995) Cardiac troponin I phosphorylation increases the rate of cardiac muscle relaxation. *Circ. Res.* **76,** 1028–1035
54. Wang, Y., Ajtai, K., and Burghardt, T. P. (2014) Ventricular myosin modifies *in vitro* step-size when phosphorylated. *J. Mol. Cell Cardiol.* **72,** 231–237
55. Colson, B. A., Locher, M. R., Bekyarova, T., Patel, J. R., Fitzsimons, D. P., Irving, T. C., and Moss, R. L. (2010) Differential roles of regulatory light chain and myosin binding protein-C phosphorylations in the modulation of cardiac force development. *J. Physiol.* **588,** 981–993
56. Hamdani, N., Bishu, K. G., von Frieling-Salewsky, M., Redfield, M. M., and Linke, W. A. (2013) Deranged myofilament phosphorylation and function in experimental heart failure with preserved ejection fraction. *Cardiovasc. Res.* **97,** 464–471
57. van der Velden, J., Narolska, N. A., Lamberts, R. R., Boontje, N. M., Borbély, A., Zaremba, R., Bronzwaer, J. G., Papp, Z., Jaquet, K., Paulus, W. J., and Stienen, G. J. (2006) Functional effects of protein kinase C-mediated myofilament phosphorylation in human myocardium. *Cardiovasc. Res.* **69,** 876–887
58. Ratti, J., Rostkova, E., Gautel, M., and Pfuhl, M. (2011) Structure and interactions of myosin-binding protein C domain C0: cardiac-specific regulation of myosin at its neck? *J. Biol. Chem.* **286,** 12650–12658
59. Petzhold, D., Simsek, B., Meissner, R., Mahmoodzadeh, S., and Morano, I. (2014) Distinct interactions between actin and essential myosin light chain isoforms. *Biochem. Biophys. Res. Commun.* **449,** 284–288
60. Toepfer, C., Caorsi, V., Kampourakis, T., Sikkel, M. B., West, T. G., Leung, M. C., Al-Saud, S. A., MacLeod, K. T., Lyon, A. R., Marston, S. B., Sellers, J. R., and Ferenczi, M. A. (2013) Myosin regulatory light chain (RLC) phosphorylation change as a modulator of cardiac muscle contraction in disease. *J. Biol. Chem.* **288,** 13446–13454
61. Trybus, K. M., and Lowey, S. (1985) Mechanism of smooth muscle myosin phosphorylation. *J. Biol. Chem.* **260,** 15988–15995
62. Ryder, J. W., Lau, K. S., Kamm, K. E., and Stull, J. T. (2007) Enhanced skeletal muscle contraction with myosin light chain phosphorylation by a calmodulin-sensing kinase. *J. Biol. Chem.* **282,** 20447–20454